

## Influence of radiation exposure on the magnetic properties of ferromagnetic/IrMn films with exchange bias

© D.O. Krivulin,<sup>1,2</sup> I.Yu. Pashenkin,<sup>1</sup> R.V. Gorev,<sup>1</sup> P.A. Yunin,<sup>1,2</sup> M.V. Sapozhnikov,<sup>1,2</sup> A.V. Grunin,<sup>3</sup> S.A. Zakharova,<sup>3</sup> V.N. Leontiev<sup>3</sup>

<sup>1</sup> Institute for Physics of Microstructures, Russian Academy of Sciences, branch of the Federal Research Center „Institute of Applied Physics of the Russian Academy of Sciences,,

603950 Nizhny Novgorod, Russia

<sup>2</sup> Lobachevsky State University,

603950 Nizhny Novgorod, Russia

<sup>3</sup> Russian Federal Nuclear Center, All-Russia Research Institute of Experimental Physics,

607188 Sarov, Russia

e-mail: ukovk@mail.ru

Received April 17, 2023

Revised April 17, 2023

Accepted April 17, 2023

In this work, the effect of the action of gamma quanta and neutrons on the magnetic properties of Ta/ferromagnet/IrMn/Ta bilayer films with an exchange bias of the hysteresis loop is studied. The samples were fabricated by magnetron sputtering, and their structure was studied by small-angle X-ray reflectometry and X-ray diffractometry. The measurement of the magnetic hysteresis loops of the irradiated and non-irradiated samples was carried out by the methods of magneto-optical Kerr magnetometry. As a result, the effect of broadening of the magnetic hysteresis loop after irradiation was found. The maximum broadening of the hysteresis loop was observed in the NiFe/IrMn film under neutron irradiation; in this case, the loop width increased by more than 2.5 times. No noticeable change in the field of the exchange bias of the hysteresis loops was observed in the entire range of radiation exposure.

**Keywords:** ferromagnetic films, radiation exposure, coercive force, exchange bias.

DOI: 10.61011/TP.2023.07.56625.72-23

### Introduction

The tunnel magnetoresistance (TMR) effect has been studied extensively over the past decade. It is utilized in the design of such devices as magnetoresistive random-access memory (MRAM) cells [1] and magnetic field sensors [2]. In its simplest form, a TMR contact consists of two ferromagnetic layers separated by an ultrathin insulating barrier. The TMR magnitude is given by  $(R_{ap} - R_p)/R_p$ , where  $R_p$  and  $R_{ap}$  are the resistances with magnetizations of magnetic layers being parallel and antiparallel. The coercive force of one of the magnetic layers should be higher for an applied magnetic field to induce an antiparallel state. This is often achieved through the use of exchange interaction with an additional sublayer of an antiferromagnetic material. A TMR magnitude of 600% [3] has been achieved at present in structures with an MgO barrier. TMR-based magnetic field sensors are used in biomagnetics [4], read-and-write heads of hard drives [5], and other applications requiring the detection of weak magnetic fields. They are characterized by a high resolution, wide operating temperature range, small size, low power consumption, and compatibility with semiconductor lithography processing. However, one important practical issue still remains uninvestigated. This issue is the radiation durability of TMR structures, which is required for their application aboard microsatellites that

provide no shielding from space radiation [6]. The influence of structural changes in an insulating barrier on electron tunneling has not been examined.

The technique of fabrication of magnetic tunnel contacts with Al<sub>2</sub>O<sub>3</sub> [7] and MgO [8] barriers has been perfected at the Institute for Physics of Microstructures of the Russian Academy of Sciences. In order to raise the coercive force of one of the ferromagnetic layers, it is deposited onto an IrMn antiferromagnetic layer. The TMRT structure thus has the following overall form: CoFeB/MgO/CoFeB/IrMn. The coercive force of a magnetic layer is enhanced due to the exchange bias effect [9], wherein effective unidirectional anisotropy arises in a ferromagnetic layer owing to the exchange interaction with an antiferromagnetic. The TMR magnitude in structures with MgO is significantly higher than in structures with an Al<sub>2</sub>O<sub>3</sub> barrier, since an MgO layer performs additional spin filtering of tunneling electrons due to the presence of a crystal texture. It is evident that the effect of radiation on the properties of a TMR structure may be associated with the emergence of defects at a ferromagnetic/barrier interface or within a barrier itself. The issue of defect formation under irradiation of a tunnel gap by heavy ions was examined in [10–12] for an Al<sub>2</sub>O<sub>3</sub> barrier and in [13,14] for MgO; electron irradiation was considered in [15]. A ferromagnetic/antiferromagnetic interface, which establishes an exchange bias in one of the ferromagnetic

layers, is another object that is affected by radiation and, in turn, may affect the operation of TMR elements. It has been determined earlier that the magnitude or the axis direction of exchange bias may vary with the dose of irradiation by He [16], C [17], and Ga [18] ions. In the present work, we examine the influence of various doses of irradiation by gamma quanta and neutrons on the magnetic properties of bilayer Co/IrMn, CoFeB/IrMn, and NiFe/IrMn ferromagnetic/antiferromagnetic films, which are used as pinned magnetic layers in TMR elements constructed in our earlier studies [7,8].

## 1. Procedure and samples

Multilayer magnetic films with unidirectional anisotropy, which are used as a pinned layer in tunnel magnetoresistive contacts, were fabricated for irradiation studies. Multilayer Ta(3)/ferromagnetic(4)/Ir<sub>20</sub>Mn<sub>80</sub>(10)/Ta(3) nanostructures (the layer thickness is indicated in nanometers) were grown on Si/SiO<sub>2</sub> substrates by high-vacuum magnetron sputtering at room temperature using an AJA-2200 setup. The chosen ferromagnetic materials were Co, Ni<sub>80</sub>Fe<sub>20</sub>, and Co<sub>40</sub>Fe<sub>40</sub>B<sub>20</sub>. Multicomponent layers were sputtered from alloyed targets of the indicated atomic composition. The residual pressure in the growth chamber did not exceed  $3 \cdot 10^{-7}$  Torr, and the working pressure of argon in the process of sputtering was  $4 \cdot 10^{-3}$  Torr for Ir<sub>20</sub>Mn<sub>80</sub> and  $2 \cdot 10^{-3}$  Torr for the other materials. Sputtering was performed in a 200 Oe external magnetic field to obtain uniaxial magnetic anisotropy of a ferromagnetic layer. The sputtering rates were as follows: NiFe: 0.09 nm/s, CoFeB: 0.08 nm/s, Co: 0.1 nm/s, IrMn: 0.03 nm/s, Ta: 0.12 nm/s.

Each of the prepared samples was divided into several parts  $\sim 7 \times 7$  mm in size, which were then irradiated at research facilities of the Russian Federal Nuclear Center – All-Russian Scientific Research Institute of Experimental Physics [19] at room temperature. One batch of samples was irradiated by reactor fission neutrons with several integral fluences and energies in excess of 0.1 MeV:  $1 \cdot 10^{14}$ ,  $5 \cdot 10^{14}$ , and  $1 \cdot 10^{15}$  cm<sup>-2</sup>. The corresponding exposure doses of associated  $\gamma$ -radiation were 0.16, 0.69, and 1.1 Mrad, respectively. Irradiation was performed in three stages in the pulsed mode with a pulse duration of  $\sim 10^{-3}$  s.

The second batch of samples was irradiated by bremsstrahlung gamma quanta produced by an LU-10-20 resonance electron accelerator. The mean quanta energy was  $\approx 1.5$  MeV, and the boundary energy was  $\approx 8$  MeV. The exposure doses for different samples were 1, 3, 5, and 8 Mrad at a mean exposure dose rate of  $10^3$  R/s. The maximum irradiation time was 2.5 h.

Structural characteristics of samples were examined by small-angle X-ray reflectometry (SAXR) and X-ray diffractometry (XRD). Experiments were performed using a Bruker D8 Discover X-ray diffractometer. SAXR curves were recorded in a „medium“ resolution setup with a Gobel Mirror and a Ge (220) double-reflection monochromator.

Diffraction patterns were measured without a monochromator to enhance the sensitivity. SAXR and XRD data were processed using the DIFFRAC.Leptos software suite and the CrystallographyOpenDatabase diffraction database.

Magnetic hysteresis loops of the obtained films were recorded using a magnetometric setup by measuring the Kerr effect in the meridional geometry with crossed polarizers. A high-stable He–Ne laser (Thorlabs HRS015B,  $\lambda = 632$  nm) served as the radiation source. It produced p-polarized monochromatic radiation that was focused onto the surface of a sample positioned in an electromagnet. The power of a reflected beam, which passed through a crossed polarizer-analyzer, was measured by a photodetector. In measurements of the magnetization loop, the angle of polarization plane rotation was taken as a function of the magnetic field. Since the samples were sufficiently thin (the overall thickness of the magnetic layer was 20 nm), their entire volume contributed to the magneto-optical Kerr effect. All measurements were performed at room temperature.

## 2. Experimental results and discussion

The typical shape of magnetic hysteresis loops before and after irradiation is presented in Figs. 1 and 2. Hysteresis loops were characterized by two parameters: exchange bias magnitude (the magnitude of the applied field corresponding to the loop center) and width. Complete sets of experimental data are presented in Tables 1 and 2. Initial films had a magnetization lying in the lateral plane. It can be seen from Figs. 1 and 2 that the parameters of magnetization loops changed significantly in the sample with a Co/IrMn magnetic layer and, to an even greater degree, in the sample with a NiFe/IrMn magnetic layer. The width of the magnetic hysteresis loop for the sample with a Co/IrMn layer increased by  $\sim 60\%$  (relative to the initial unirradiated sample) at a  $\gamma$ -exposure dose of 5 Mrad. The position of the loop center varied within 8 Oe in this case. The results of previous measurements performed using the same setup suggest that the exchange bias field for ferromagnetic/antiferromagnetic structures may vary by up to 10 Oe depending on the sample position. This spread is attributable to a nonuniform field distribution within an electromagnet gap and to the probable variation of material parameters over the sample area. The observed variations of the loop center position are within the accuracy of the experiment. The maximum loop width under neutron irradiation was observed at a fluence of  $5 \cdot 10^{14}$  cm<sup>-2</sup> (the loop width increased by  $\sim 33\%$  relative to the initial sample); no appreciable variation of the exchange bias field magnitude was detected in this case. The effect of irradiation was the most pronounced in films with a ferromagnetic NiFe layer. The maximum change in the loop width under irradiation by  $\gamma$ -quanta at an exposure dose of 5 Mrad was  $\sim 136\%$  relative to the initial sample. This loop broadening effect was even more significant under irradiation by neutrons (and, consequently, associated

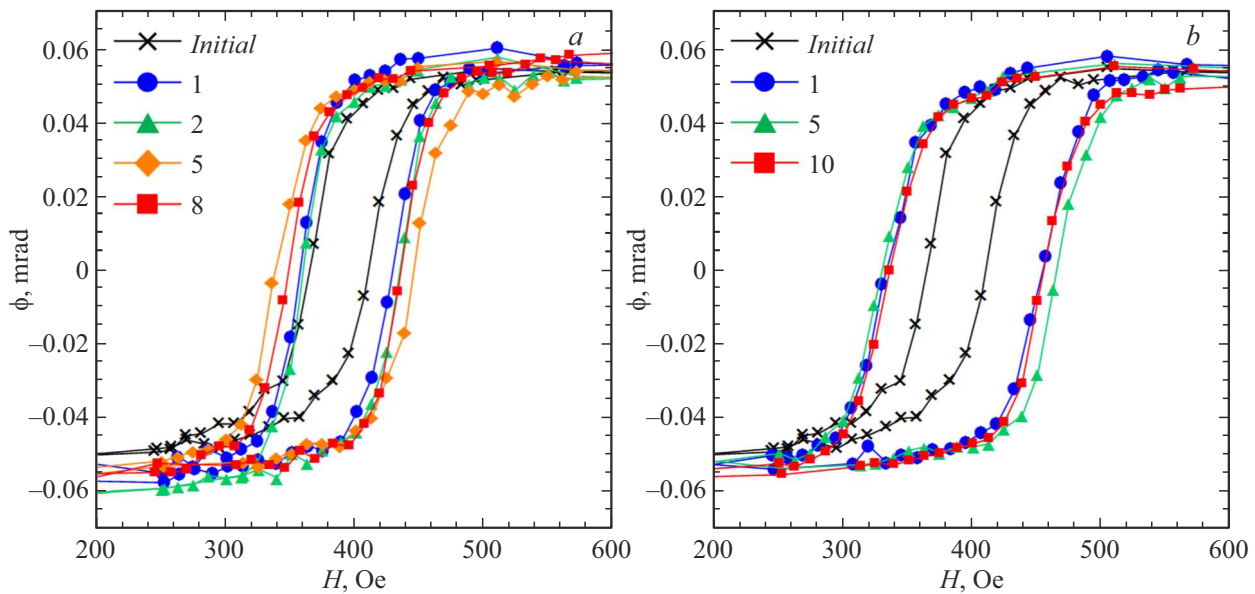


**Figure 1.** Magnetic hysteresis loops of a NiFe/IrMn film: *a* — after irradiation by  $\gamma$ -quanta (exposure doses are indicated in Mrad), *b* — under irradiation by neutrons (fluences are indicated in  $10^{14} \text{ cm}^{-2}$ ).

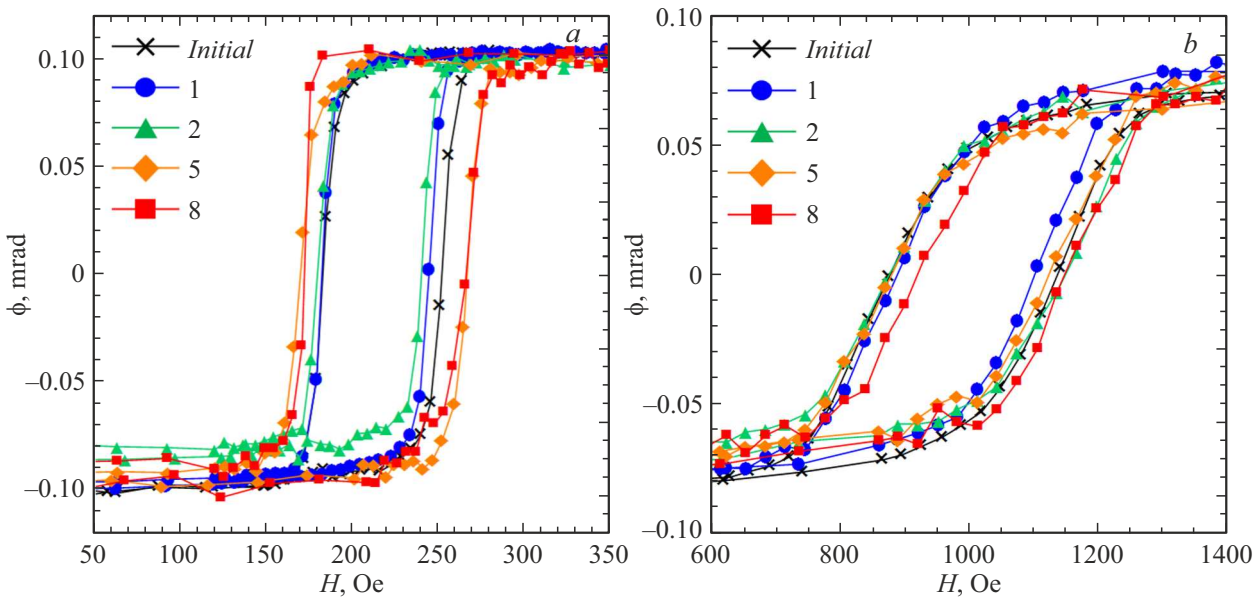


**Figure 2.** Magnetic hysteresis loops of Co/IrMn (*a*) and CoFe/IrMn (*b*) films after irradiation by  $\gamma$ -quanta (exposure doses are indicated in Mrad).

gamma quanta): the width changed by almost 200%. The magnitude of the exchange bias field did not undergo any significant variation within the entire range of neutron fluences. It is worth noting that the hysteresis loop broadened with increasing irradiation dose in all samples, but contracted somewhat at the highest levels (an exposure dose of 8 Mrad for bremsstrahlung radiation and a neutron fluence of  $10^{15} \text{ cm}^{-2}$  with associated irradiation by gamma quanta with an exposure dose of 0.5 Mrad). Additional measurements at high irradiation doses and different neutron spectra are needed to determine whether this is a stable

trend and what are the reasons behind it. It is important from a practical standpoint that structures with a CoFeB ferromagnetic layer are the least affected by irradiation and hold the most promise for application in TMR elements.

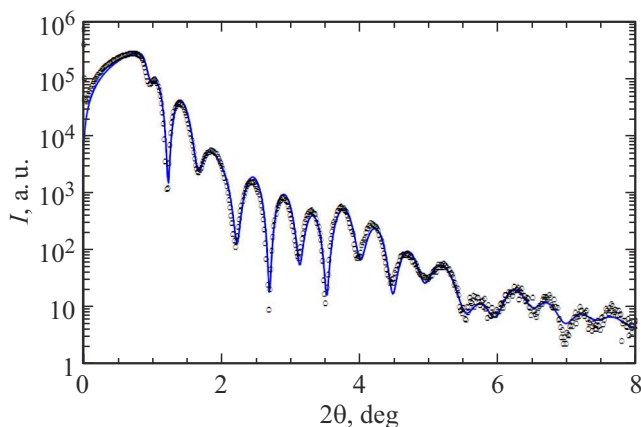
As was noted in [20], changes in the parameters of a magnetic hysteresis loop are induced by the formation of interstitial point defects and vacancies (nuclear defects) under irradiation. In view of this, the structure of samples was examined with a diffractometer. Figure 3 shows the SAXR curve of the initial sample (Ta(5)/IrMn(10)/NiFe(4)/Ta(3)/Si) prior to irradiation. Ex-

**Table 1.** Dependence of the parameters of magnetic hysteresis loops on the exposure dose of bremsstrahlung radiation

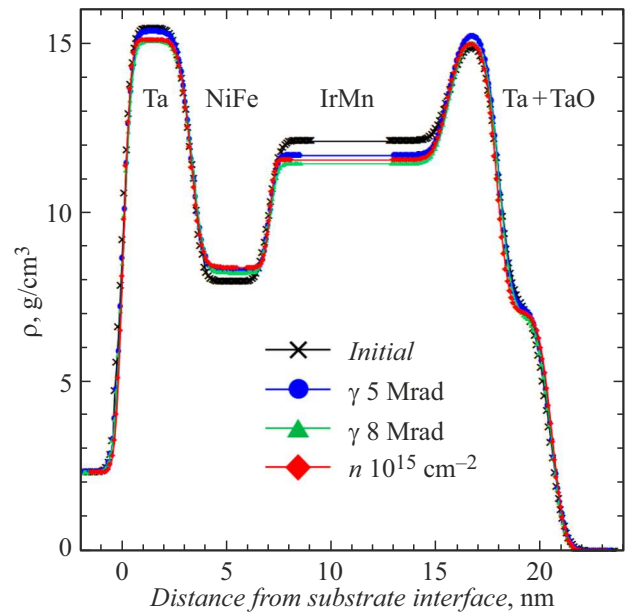
Dose (Mrad)		0	1	2	5	8
Co/IrMn	Width, Oe	69.4	62.4	60.5	97.2	94.2
	Exchange bias field, Oe	217.3	213.3	209.9	218.1	218
CoFeB/IrMn	Width, Oe	258.6	212.7	274	244.3	227.4
	Exchange bias field, Oe	1008.7	996.7	1015	1002.9	1035.3
NiFe/IrMn	Width, Oe	45.6	71.8	75.4	107.8	87
	Exchange bias field, Oe	388.1	393.7	397.5	391.9	392.2

**Table 2.** Dependence of the parameters of magnetic hysteresis loops on the neutron fluence after irradiation by reactor neutrons

Neutron fluence, $10^{14} \text{ cm}^{-2}$		0	1	5	10
Co/IrMn	Width, Oe	69.4	82.2	92.7	82.5
	Exchange bias field, Oe	217.3	211.1	209.9	227.3
CoFeB/IrMn	Width, Oe	258.6	289.2	274.1	257.3
	Exchange bias field, Oe	1008.7	995.4	1056	960.4
NiFe/IrMn	Width, Oe	45.6	121.4	135.6	119.3
	Exchange bias field, Oe	388.1	394.3	398	396

**Figure 3.** Measured (open circles) and numerically calculated (blue curve (in the online version)) SAXR curves of the initial non-irradiated Ta/NiFe/IrMn/Ta sample.

perimental data area characterized well by the model of a multilayer structure. Similar measurements were also performed for samples exposed to bremsstrahlung radiation

**Figure 4.** Profiles of the distribution of density over depth for the Ta/NiFe/IrMn/Ta structure before and after exposure to various types of radiation (black crosses — before irradiation, blue circles (in the online version) — after irradiation by gamma quanta with a dose of 5 Mrad, green triangles (in the online version) — after irradiation by gamma quanta with a dose of 8 Mrad, red diamonds (in the online version) — after irradiation by neutrons with a fluence of  $10^{15} \text{ cm}^{-2}$ ).

(the irradiation dose was 5 and 8 Mrad) and gamma-neutron radiation with a neutron fluence of  $1 \cdot 10^{15} \text{ cm}^{-2}$ . Attenuation of the contrast of interference oscillations was observed in experiments. This is normally caused by suppression of a jump in electron density between layers or broadening of interfaces. The profiles of distribution of electron (and, consequently, mass) density in all the studied structures were reconstructed by fitting the model curves to experimental ones. The obtained profiles are compared in Fig. 4. A systematic suppression of the density difference between IrMn and NiFe layers, which may induce the observed attenuation of contrast of oscillations, is evident in Fig. 4.

Figure 5 shows the diffraction pattern of the initial non-irradiated NiFe/IrMn sample. Peaks of the (111) IrMn FCC phase and the (011) NiFe BCC phase are seen clearly. The second reflection order (peaks (222) and (022), respectively) is also visible. The peak around 69 deg is a trace of the (004) silicon substrate peak. In order to get rid of an intense peak from a single-crystal substrate, a detuning of 1 deg in angle  $\omega$  from the normal to the surface was set in scanning. The (111) IrMn peak has a characteristic shape and is surrounded by thickness contrast oscillations, which are indicative of a fine crystal layer quality. At the very least, very strong texturing of IrMn crystallites by plane (111) parallel to the substrate occurs, with the vertical size of IrMn coherence regions being consistent

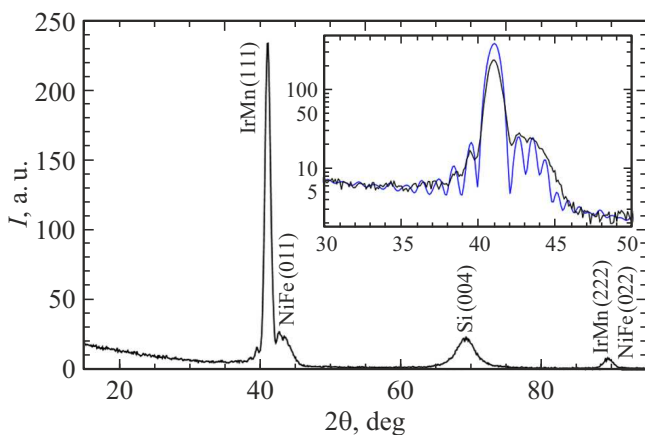


**Figure 5.** Diffraction pattern of the initial non-irradiated Ta/NiFe/IrMn/Ta sample.

with the layer thickness. Similar weaker oscillations are discernible around the NiFe peak. The results of fitting (inset in Fig. 5) allow one to determine the thickness of crystal blocks in the corresponding layers (9 nm for IrMn and 4 nm for NiFe), which agrees with reflectometry data and growth specifications.

The diffraction patterns of samples subjected to various types of irradiation in the experiment did not differ from the initial one. This suggests that the crystal structure of samples remains essentially undamaged and the observed effects are associated mostly with suppression of the density jump between layers (presumably, induced by mixing of materials at the boundary of films under irradiation).

Thus, the position of the center of a magnetic hysteresis loop (exchange bias field) did not undergo any significant shifts within the experimental accuracy (20 Oe). A general trend in the behavior of a magnetic hysteresis loop is its broadening with increasing irradiation dose. The loop width reached its maximum at a certain dose (in the present case, 5 Mrad under irradiation by  $\gamma$ -quanta and  $5 \cdot 10^{14} \text{ cm}^{-2}$  under neutron irradiation) and leveled off at higher doses. We suspect that the loop width variation is attributable to a change in the density jump between layers due to material mixing under irradiation. In the case of application of such structures in TMR elements, the effect of magnetization loop broadening will lead to a change (contraction) of the range of fields within which ferromagnetic layers undergo remagnetization. Note that although the coercive force magnitude increases considerably after irradiation, it is still much ( $\sim 4$ – $9$  times) weaker than the exchange bias field. Thus, the remagnetization loops of free and pinned layers in a TMR cell will remain spaced apart on the external magnetic field scale and will not overlap. Therefore, a TMR cell should retain its functionality under the examined irradiation doses.

## Conclusion

The effect of gamma quanta and neutrons with a relatively high energy on the magnetic properties of Co/IrMn,  $\text{Ni}_{80}\text{Fe}_{20}/\text{IrMn}$ , and  $\text{Co}_{40}\text{Fe}_{40}\text{B}_{20}/\text{IrMn}$  films fabricated by magnetron sputtering was revealed. It was demonstrated that the magnetic hysteresis loop broadens with increasing irradiation „dose“. The maximum width of the magnetic hysteresis loop corresponds to a dose of 5 Mrad for bremsstrahlung  $\gamma$ -quanta with a mean energy of 1.5 MeV and to a fluence of  $5 \cdot 10^{14} \text{ cm}^{-2}$  for fission neutrons and associated gamma radiation with a dose of 0.69 Mrad. We attribute this loop broadening to partial mixing of layer materials at the boundary of films, which is characterized by a suppression of the jump in electron density between magnetic layers. The position of the loop center relative to zero (exchange bias field) turned out to be insensitive to irradiation with the examined parameters. This is indicative of a high radiation resistance of the studied ferromagnetic films.

## Funding

The irradiation of samples and the examination of their magnetic and structural properties were performed as part of the scientific program of the National Center of Physics and Mathematics, section No. 6 „Nuclear and Radiation Physics“. The sample fabrication procedure was validated under the state assignment of the Institute of Applied Physics of the Russian Academy of Sciences (project 0030-2021-0021). Equipment provided by the „Physics and Technology of Micro- and Nanostructures“ common use center (Institute for Physics of Microstructures of the Russian Academy of Sciences) was used in the study.

## Conflict of interest

The authors declare that they have no conflict of interest.

## References

- [1] S. Yuasa, D.D. Djayaprawira. *J. Phys.*, **40**, 337 (2007). DOI: 10.1088/0022-3727/40/21/R01
- [2] P.P. Freitas, R. Ferreira, S. Cardoso. *IEEE Trans. Magn.*, **104** (10), 1894 (2016). DOI: 10.1109/JPROC.2016.2578303
- [3] S. Ikeda, J. Hayakawa, Y. Ashizawa, Y.M. Lee, K. Miura, H. Hasegawa, M. Tsunoda, F. Matsukura, H. Ohno. *Appl. Phys. Lett.*, **93**, 082508 (2008).
- [4] S.G. Grancharov, H. Zeng, S. Sun, S.X. Wang, S. O'Brien, C.B. Murray, J.R. Kirtley, G.A. Held. *J. Phys. Chem.*, **109**, 13030 (2005).
- [5] M. Sining, C. Yonghua, L. Feng, C. Xingfu, X. Bin, L. Puling, M. Patwari, X. Haiwen, C. Clif, B. Miller, D. Menard, B. Pant, J. Loven, K. Duxstad, L. Shaoping, Z. Zhengyong, A. Johnston, R. Lamberton, M. Gubbins, T. McLaughlin, J. Gadbois, D. Juren, B. Cross, X. Song, P. Ryan. *IEEE Trans. Magn.*, **42** (2), 97 (2006). DOI: 10.1109/TMAG.2005.861788

- [6] A. Edelstein. Magnetoresistivesensors, *J. Phys. Condens. Matter*, **19**, 165217 (2007). DOI: 10.1088/0953-8984/19/16/165217
- [7] I.Yu. Pashen'kin, M.V. Sapozhnikov, N.S. Gusev, V.V. Rogov, D.A. Tatarskiy, A.A. Fraerman. *Tech. Phys.*, **64**(11), 1642 (2019). DOI: 10.21883/JTF.2019.11.48336.122-19
- [8] I.Yu. Pashen'kin, M.V. Sapozhnikov, N.S. Gusev, V.V. Rogov, D.A. Tatarskii, A.A. Fraerman, M.N. Volochaev. *JETP Lett.*, **111**, 690 (2020).
- [9] W.H. Meiklejohn, C.P. Bean. *Phys. Rev.*, **105** (3), 904 (1957). DOI: 10.1103/physrev.105.904
- [10] Y. Conraux, J.P. Nozières, V.Da Costa, M. Toulemonde, K. Ounadjela. *J. Appl. Phys.*, **93**, 7301 (2003). DOI: 10.1063/1.1558659
- [11] T. Som, T. Kanjilal, D. Moodera, J.S. Eur. *Phys. J. Appl. Phys.*, **32**, 115 (2005). DOI: 10.1051/epjap:2005080
- [12] J.C.A. Huang, C.Y. Hsu, Y.F. Liao, M.Z. Lin, C.H. Lee. *J. Appl. Phys.*, **98**, 103504 (2005). DOI: 10.1063/1.2132096
- [13] J.-Y. Park, J.-M. Kim, J. Ryu, J. Jeong, B.-G. Park. *Thin Solid Films*, **686**, 137432 (2019). DOI: 10.1016/j.tsf.2019.137432
- [14] B.M.S. Teixeira, A.A. Timopheev, N. Caçoilo, L. Cuchet, J. Mondaud, J.R. Childress, S. Magalhaes, E. Alves, N.A. Sobolev. *J. Phys., D: Appl. Phys.*, **53**, 455003 (2020). DOI: 10.1088/1361-6463/aba38c
- [15] Y. Zhang, Y.Z. Wang, X.F. Han, H. Deng, H. Huang, J.H. Guo, Y. Liang, W.R. Si, A.F. Jiang, H.F. Liu, J.F. Feng, C.H. Wan, L. Yin, G.Q. Yu, *J. Magn. Magn. Mater.*, **563**, 169954 (2022).
- [16] D. Schafer, J. Geshev, S. Nicolodi, L.G. Pereira, J.E. Schmidt, P.L. Grande. *Appl. Phys. Lett.*, **93**, 042501 (2008).
- [17] C.H. Yang, Chih-Huang Lai, S. Mao. *J. Appl. Phys.*, **93**, 6596 (2003).
- [18] Qi Xian-Jin, Wang Yin-Gang, Miao Xue-Fei, Li Zi-Quan, Huang Yi-Zhong. *Chin. Phys. B*, **20**, 057503 (2011). DOI: 10.1088/1674-1056/20/5/057503
- [19] N.V. Zavialov, *UFN*, **192** (5), 547 (2022).
- [20] D. Schafer, P.L. Grande, L.G. Pereira, J. Geshev. *J. Appl. Phys.*, **109**, 023905 (2011). DOI: 10.1063/1.3532044

*Translated by D.Safin*